A Study on Free Vibration of a Spinning Disk

Jintai Chung*, Nam-Chel Kang and Jang Moo Lee*****

(Received March 2, 1995)

Without a logical jump, we have derived the governing equation for free vibration of a spinning circular disk by using the variational formulation based upon the Kirchhoff plate theory and von Karman strain one. It has been found during the derivation that the governing equation is theoretically valid under the assumption that in-plane deflections are steady and axisymmetric, and that internal forces are linearized while the strains remain nonlinear. The natural frequencies and the critical speeds of a freely spinning disk are obtained approximately and their dependencies on the spinning speed, mode number, and natural frequency of the stationary disk are analyzed.

Key Words: Spinning Circular Disk, Transverse Vibration, Natural Frequency, Critical Speed

1. Introduction

Vibrations and stability of spinning circular disks have been continually studied and discussed for a long time since Lamb and Southwell (Lamb, 1921) initiated the study, because their application area has not only been widen from a circular saw to computer floppy/hard disks but also the problems are fascinating themselves with respect to physical nature. Early studies put a focus on free vibrations and critical speeds of flexible spinning disks (Mote, 1965, Eversman, 1969, Adams, 1987). Researches on circular disks moved toward the responses and stability of stationary disks with moving or rotating loads: e. g., Mote, 1970 and Shen, 1993. On the other hand, practical problems such as a guided circular saw and a head-disk interface in a computer hard disk became popular topics in industries, many researches have been carried out on the dynamic responses and stability of spinning disks with a transverse load system (Iwan, 1976, Benson, 1978, Hutton, 1987, Ono, 1991, Chen, 1992).

When the dynamic characteristics of spinning disks were analyzed in most of previous studies (e. g., Iwan, 1976, Benson, 1977, Hutton, 1987 and Adams, 1987), the governing equation for the transverse deflection (or out-of-plane deflection) of the disks was derived by adding the inertial term to the Kirchhoff plate equation and then using a transformation from the rotating coordinate system to the space-fixed coordinate system. However, even if the resultant governing equation is correct, this approach is somewhat inappropriate because it seems that the coordinate transformation results in different governing equations. Accepting this approach makes a mistake to assert that the system characteristics, i. e., the eigenvalues of a spinning disk depend upon the coordinate system to be used. Probably for this reason, it seems that Mote studied stationary circular disks with moving loads instead of spinning circular ones with stationary loads (Mote, 1965 and 1970).

Without loss of generality, in this study, the governing equation is derived from the variational formulation based on the Kirchhoff plate theory and von Karman strain theory. In addition, we scrutinize assumptions including linearizations which are used in driving the equations.

* Department of Mechanical Engineering, Hanyang University in Ansan
** R&D Center, Hankook Tire Mfg. Co., Ltd.
*** Department of Mechanical Design and Production Engineering, Seoul National University

When the Galerkin approximation is applied to obtain the eigenvalue problem, in order to reduce calculation complexity, we use the zero nodal circle modes which are chosen as simple comparison functions of the radial coordinate. Moreover, approximate calculation of the natural frequencies and critical speeds is presented without the eigenvalue search of numerical analyses. Finally, dependency of the natural frequencies and critical speeds on the spinning speed and radial modes is also studied .

2. Derivation of the Governing Equation

The disk, as shown in Fig. 1, is fixed at the inner radius a and free at the outer radius b ; the material of the disk is isotropic and elastic; the thickness and the rotating speed of the disk are h and Ω, respectively. The X-Y coordinate system is fixed in space while the vectors e_r and e_θ are rotating with the disk. Hence the coordinate θ is measured with respect to the space-fixed coordinate system.

The Kirchhoff plate theory gives us the following equations which define the relation between the displacements:

$$u_r(r,\ \theta,\ z,\ t) = \bar{u}_r(r,\ \theta,\ t) - z\frac{\partial w(r,\ \theta\ t)}{\partial r} \tag{1}$$

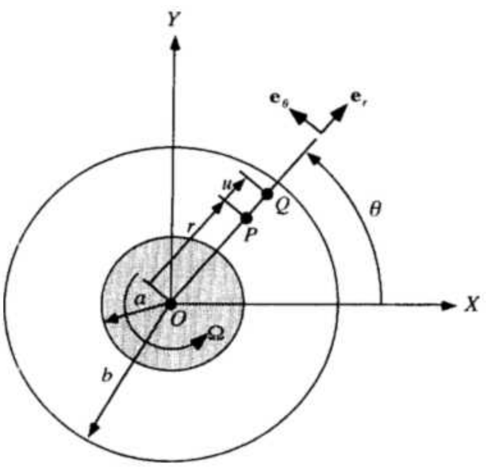

Fig. 1 Configuration of a spinning disk.

$$u_\theta(r,\ \theta,\ z,\ t) = \bar{u}_\theta(r,\ \theta,\ t) - z\frac{\partial w(r,\ \theta,\ t)}{r\partial\theta} \tag{2}$$

$$u_z(r,\ \theta,\ z,\ t) = w(r,\ \theta,\ t) \tag{3}$$

where u_r, u_θ and u_z are the displacements at an arbitrary point inside the plate in the r, θ and z-directions, respectively, while $\bar{u}_r$, $\bar{u}_\theta$ and w are the displacements of a point on the middle surface of the plate. If a transverse load is not applied on the disk, it is plausible to assume that the in-plane deflections are steady and axisymmetric. The assumption reduces the in-plane displacements to

$$\bar{u}_r(r,\ \theta,\ t) = u(r) \tag{4}$$

$$\bar{u}_\theta(r,\ \theta,\ t) = 0 \tag{5}$$

which means that the radial displacement is a function of only the radial coordinate and that there is no circumferential displacement. Many studies adopted the governing equation which was derived using the assumption that the in-plane deflection is steady and axisymmetric, even in case that a transverse load is applied to the spinning disk. Strictly speaking, however, the in-plane deflection is no longer steady and axisymmetric when the spinning disk has a transverse load. Since a transverse load breaks steady state and axisymmetricity, the in-plane displacements given by Eqs. (4) and (5) may not be valid any longer in this case. Therefore, it is reasonable that the assumption is used in case of a freely spinning disk without a transverse load.

Considering geometric nonlinearity, this study uses the simplified von Karman strain theory which may be expressed as the following nonlinear displacement-strain relations:

$$\varepsilon_r = \frac{\partial u_r}{\partial r} + \frac{1}{2}\left(\frac{\partial u_z}{\partial r}\right)^2 \tag{6}$$

$$\varepsilon_\theta = \frac{u_r}{r} + \frac{\partial u_\theta}{r\partial\theta} + \frac{1}{2}\left(\frac{\partial u_z}{r\partial\theta}\right)^2 \tag{7}$$

$$\varepsilon_{r\theta} = \frac{1}{2}\left(\frac{\partial u_r}{r\partial\theta} + \frac{\partial u_\theta}{\partial r} - \frac{u_\theta}{r} + \frac{\partial u_z}{\partial r}\frac{\partial u_z}{r\partial\theta}\right) \tag{8}$$

Since the disk is typically thin, the stresses σ_z, σ_{zr} and $\sigma_{\theta z}$ are assumed negligible, i. e.,

$$\sigma_z = \sigma_{zr} = \sigma_{\theta z} = 0 \tag{9}$$

For a homogeneous, elastic and Hookean

material, the stress-strain relations are given by

$$\sigma_r = \frac{E}{1-v^2}(\varepsilon_r + v\varepsilon_\theta) \tag{10}$$

$$\sigma_\theta = \frac{E}{1-v^2}(v\varepsilon_r + \varepsilon_\theta) \tag{11}$$

$$\sigma_{r\theta} = \frac{E}{1+v}\varepsilon_{r\theta} \tag{12}$$

where E is Young's modulus and v is Poisson's ratio.

Based on the above assumptions, the strain energy denoted by U is represented by

$$U = \frac{1}{2}\int_V (\sigma_r\varepsilon_r + \sigma_\theta\varepsilon_\sigma + 2\sigma_{r\theta}\varepsilon_{r\theta})\, dV \tag{13}$$

where V is the volume of the disk. Integrating the term in the parentheses of Eq. (13) from $-h/2$ to $h/2$ with respect to z, the strain energy can be rewritten by

$$U = \frac{1}{2}\int_A (Q_r\bar{\varepsilon}_r + Q_\theta\bar{\varepsilon}_\theta + Q_{r\theta}\bar{\varepsilon}_{r\theta} - M_r\chi_r - M_\theta\chi_\theta - M_{r\theta}\chi_{r\theta})\, dA \tag{14}$$

where A is the area of the disk; $\bar{\varepsilon}_r$, $\bar{\varepsilon}_\theta$ and $\bar{\varepsilon}_{r\theta}$ are the strains at the middle surface; χ_r, χ_θ and $\chi_{r\theta}$ are the curvature changes of the deflected middle surface; Q_r, Q_θ and $Q_{r\theta}$ are the internal forces per unit length of the middle surface; M_r, M_θ and $M_{r\theta}$ are the internal moments per unit length of the middle surface:

$$\left.\begin{aligned} \varepsilon_i &= \bar{\varepsilon}_i - z\chi_i \\ Q_i &= \int_{-h/2}^{h/2} \sigma_i dz \\ M_i &= \int_{-h/2}^{h/2} z\sigma_i dz \end{aligned}\right\}, \quad i = r,\ \theta,\ r\theta \tag{15}$$

It is noted that the strains $\bar{\varepsilon}_r$, $\bar{\varepsilon}_\theta$ and $\bar{\varepsilon}_{r\theta}$ are nonlinear functions of the displacements while the curvature changes χ_r, χ_θ and $\chi_{r\theta}$ are linear functions. Similarly, the internal forces Q_r, Q_θ and $Q_{r\theta}$ are nonlinear functions while the internal moments M_r, M_θ and $M_{r\theta}$ are linear functions.

Linearizations of the strains or internal forces have a great effect on the governing equations and their solutions. We consider here three cases which seem physically meaningful.

1. When both the strains and internal forces are linearized, the governing equation of the in-plane deflection is completely decoupled with that of the out-of-plane deflection. In this case the in-plane stresses do not have any influence on the out-of-plane deflection.
2. When only the internal forces are linearized, the in-plane deflection are coupled with the out-of-plane deflection so the in-plane stresses have an influence on the out-of-plane deflection. However, the governing equation of the in-plane deflection is expressed in terms of only the in-plane displacement and it can be easily solved. This benefit leads to the most wide use of the governing equations derived by using this linearization.
3. When none of them are linearized, the equations of the in-plane and out-of-plane deflections become totally coupled nonlinear differential equations. They should be solved by numerical approaches which are very cumbersome; hence, we circumvent further discussion on it in this study.

More detailed investigation on the first and second cases is given the next section. First of all, we derive the governing equations using the second case of linearization.

The kinetic energy of the spinning disk is required to obtain the governing equations by using Hamilton's principle. The velocity of an arbitrary point shown in Fig. 1 can be denoted by

$$\boldsymbol{v} = \bar{\boldsymbol{v}} - z\boldsymbol{\Psi} \tag{16}$$

where

$$\bar{\boldsymbol{v}} = \Omega(r+u)\,\boldsymbol{e}_\theta + \left[\frac{\partial w}{\partial t} + \Omega(r+u)\frac{\partial w}{r\partial\theta}\right]\boldsymbol{e}_z \tag{17}$$

$$\boldsymbol{\Psi} = \left(\frac{\partial^2 w}{\partial t\partial r} - \Omega\frac{\partial w}{r\partial\theta}\right)\boldsymbol{e}_r + \left(\frac{\partial^2 w}{r\partial t\partial\theta} + \Omega\frac{\partial w}{\partial r}\right)\boldsymbol{e}_\theta \tag{18}$$

Since the height of disk is small, the kinetic energy of the spinning disk may be given by

$$T = \frac{1}{2}\rho h\int_A \bar{\boldsymbol{v}}\cdot\bar{\boldsymbol{v}}\, dA \tag{19}$$

where ρ is the density of the disk. When calculating the kinetic energy expressed in Eq. (19), we neglect the higher-order nonlinear terms and we use the fact that u is much smaller than r.

In order to obtain the governing equations, we use Hamilton's principle which is expressed by

$$\delta\int_{t_1}^{t_2}(T-U)\,dt=0 \tag{20}$$

where t_1 and t_2 are arbitrary times. From Eq. (20), the governing equations are obtained as

$$\frac{dq_r}{dr}+\frac{q_r-q_\theta}{r}=-r \tag{21}$$

$$\rho h\left(\frac{\partial^2 w}{\partial t^2}+2\Omega\frac{\partial^2 w}{\partial t\partial\theta}+\Omega^2\frac{\partial^2 w}{\partial\theta^2}\right)$$
$$+D\nabla^4 w-\rho h\Omega^2\left[\frac{\partial}{r\partial r}\left(rq_r\frac{\partial w}{\partial r}\right)\right.$$
$$\left.+\frac{\partial}{r\partial\theta}\left(q_\theta\frac{\partial w}{r\partial\theta}\right)\right]=0 \tag{22}$$

where

$$q_i=\frac{Q_i^{lin}}{\rho h\Omega^2},\ i=r,\ \theta \tag{23}$$

$$D=\frac{Eh^3}{12(1-v^2)} \tag{24}$$

$$\nabla^4=\nabla^2\nabla^2$$
$$=\left(\frac{\partial^2}{\partial r^2}+\frac{1}{r}\frac{\partial}{\partial r}+\frac{1}{r^2}\frac{\partial^2}{\partial\theta^2}\right)^2 \tag{25}$$

in which Q_r^{lin} and Q_θ^{lin} are the linearized internal forces of Q_r and Q_θ, respectively. The boundary conditions are given by

$$u=w=\frac{\partial w}{\partial r}=0 \text{ at } r=a \tag{26}$$

$$Q_r^{lin}=D\frac{\partial}{\partial r}\nabla^2 w-\frac{\partial M_{r\theta}}{r\partial\theta}$$
$$=M_r=0 \text{ at } r=b \tag{27}$$

It is noted that Eq. (21) contains only the in-plane displacement . Therefore, using the boundary conditions given in Eq. (26) and (27), Eq. (21) can be easily solved with a closed form by Hutton.(1987)

3. Analysis of Free Vibration of the Spinning Disk

The Galerkin method is used in this study to investigate the transverse free vibration of the spinning disk. Since the natural frequencies of the stationary disk for all modes with one or more nodal circles are greater than those of modes with zero nodal circles and up to three or four nodal diameters, the present analysis includes only modes with zero nodal circles (Iwan, 1976). Based on this assumption, we express the transverse displacement as

$$w(r,\ \theta,\ t)=\sum_{n=0}^{N}[C_n(t)\cos n\theta+S_n(t)\sin n\theta]R_n(r) \tag{28}$$

where n is the number of nodal diameters and N is the total number of nodal diameters to be used in Galerkin approximation. Using Eq. (28), the corresponding boundary conditions are reduced to

$$R_n=\frac{dR_n}{dr}=0 \text{ at } r=a \tag{29}$$

$$\left.\begin{aligned}&\frac{d}{dr}(\tilde{\nabla}_n^2 R_n)-(1-v)\frac{n^2}{r^2}\left(\frac{dR_n}{dr}-\frac{R_n}{r}\right)=0\\&\frac{d^2R_n}{dr^2}+\frac{v}{r}\left(\frac{dR_n}{dr}-n^2\frac{R_n}{r}\right)=0\end{aligned}\right\} \text{ at } r=b \tag{30}$$

where

$$\tilde{\nabla}_n^2=\frac{d^2}{dr^2}+\frac{1}{r}\frac{d}{dr}-\frac{n^2}{r^2} \tag{31}$$

For simplicity of calculation, the function may be normalized by the following condition:

$$\pi\rho h\int_a^b R_n^2 r\,dr=1,\quad n=0,\ 1,\ \cdots,\ N \tag{32}$$

Moreover, R_n is assumed as the following comparison function:

$$R_n(r)={}_1C_n(r-a)^2+{}_2C_n(r-a)^3$$
$$+{}_3C_n(r-a)^4 \tag{33}$$

where ${}_1C_n$, ${}_2C_n$ and ${}_3C_n$ are to be determined by the boundary conditions Eq. (30) and the normalization condition Eq. (32). Note that R_n, given in Eq. (33), automatically satisfies the geometric boundary conditions of Eq. (29).

After multiplying the both sides of Eq. (22) by $(\cos n\theta)R_n$ or $(\sin n\theta)R_n$, integrating it over the area A and using the orthogonal properties of cosine and sine functions as well as the normalization condition, we can obtain the following discrete equations:

$$\ddot{C}_n+2n\Omega\dot{S}_n+[{}_s\omega_n^2-\Omega^2(n^2$$
$$-\alpha_n-n^2\beta_n)]C_n=0,\ n=0,\ 1,\ \cdots,\ N \tag{34}$$

$$\ddot{S}_n-2n\Omega\dot{C}_n+[{}_s\omega_n^2-\Omega^2(n^2$$
$$-\alpha_n-n^2\beta_n)]S_n=0,\ n=1,\ 2,\ \cdots,\ N \tag{35}$$

where ${}_s\omega_n$ is the natural frequency of the n nodal diameter mode when the disk is stationary or $\Omega=0$; α_n and β_n are nondimensional parameters related with the in-plane forces:

$$_s\omega_n=\left[\pi D\int_a^b(\tilde{\nabla}_n^4 R_n)R_n r dr)\right]^{1/2} \quad (36)$$

$$\alpha_n=-\pi\rho h\int_a^b\frac{d}{dr}\left(rq_r\frac{dR_n}{dr}\right)R_n dr \quad (37)$$

$$\beta_n=\pi\rho h\int_a^b q_\theta\frac{R_n^2}{r}dr \quad (38)$$

in which

$$\tilde{\nabla}_n^4=\tilde{\nabla}_n^2\tilde{\nabla}_n^2 \quad (39)$$

The discrete equations defined by Eqs. (34) and (35) can be written in a matrix-vector form of

$$\ddot{\boldsymbol{x}}+\boldsymbol{A}\dot{\boldsymbol{x}}+\boldsymbol{B}\boldsymbol{x}=\boldsymbol{0} \quad (40)$$

where $\boldsymbol{A}$ is a $(2N+1)\times(2N+1)$ skew-symmetric matrix, $\boldsymbol{B}$ is a $(2N+1)\times(2N+1)$ diagonal matrix, and $\boldsymbol{x}$ is a $(2N+1)\times 1$ vector expressed as

$$\boldsymbol{x}=\{\boldsymbol{y}_0,\ \boldsymbol{y}_1,\ \cdots,\ \boldsymbol{y}_N\}^T \quad (41)$$

in which

$$\boldsymbol{y}_0=\{C_0\},\ \boldsymbol{y}_n=\{C_n,\ S_n\},\quad n=1,\ 2,\ \cdots,\ N \quad (42)$$

The eigenvalue problem of Eq. (40) results in the characteristic equation which is factored as the following:

$$\det(s^2\boldsymbol{I}+s\boldsymbol{A}+\boldsymbol{B})=\det(\boldsymbol{w}_0)\det(\boldsymbol{w}_1)\cdots\det(\boldsymbol{w}_N)=0 \quad (43)$$

where

$$\boldsymbol{w}_0=[s^2+{}_s\omega_0^2+\Omega^2\alpha_0] \quad (44)$$

$$\boldsymbol{w}_n=\begin{bmatrix}s^2+{}_s\omega_n^2-\Omega^2(n^2-\alpha_n-n^2\beta_n) & 2n\Omega s\\ -2n\Omega s & s^2+{}_s\omega_n^2-\Omega^2(n^2-\alpha_n-n^2\beta_n)\end{bmatrix},\ n=1,\ 2,\ \cdots,\ N \quad (45)$$

Since the characteristic equation, as shown in Eq. (43), is factored into simple equations, the natural frequencies can be expressed as

$$_f\omega_n=\left|\sqrt{{}_s\omega_n^2+\Omega^2(\alpha_n+n^2\beta_n)}+n\Omega\right|\quad n=0,\ 1,\ \cdots,\ N \quad (46)$$

$$_r\omega_n=\left|\sqrt{{}_s\omega_n^2+\Omega^2(\alpha_n+n^2\beta_n)}-n\Omega\right|\quad n=0,\ 1,\ \cdots,\ N \quad (47)$$

where $_f\omega_n$ and $_r\omega_n$ are the natural frequencies of the nodal diameter mode for the forward and backward traveling waves, respectively.

The critical speed is defined as the speed when the natural frequency for the reversed traveling wave is equal to zero. The critical speed with nodal diameters, denoted by $_c\Omega_n$, can be easily calculated from Eq. (47) only when $n^2-\alpha_n-n^2\beta_n$ is greater than zero:

$$_c\Omega_n=\frac{{}_s\omega_n}{\sqrt{n^2-\alpha_n-n^2\beta_n}}\quad n^2-\alpha_n-n^2\beta_n>0 \quad (48)$$

If $n^2-\alpha_n-n^2\beta_n$ is equal to zero or less than zero, there exists no critical speed. Once we know the values of $_s\omega_n$, α_n and β_n, the natural frequencies and the critical speeds become functions of Ω. Therefore, there is no need to calculate the eigenvalues with numerical approaches. See the natural frequencies defined in Eqs. (46) and (47) and the critical speed defined in Eq. (48).

Let us now consider the case that both the strains and internal forces are linearized. In this case, the equation of the transverse deflection is completely decoupled with that of the in-plane deflection so the internal force terms, q_r and q_θ (namely, α_n and β_n), disappear in the governing Eq. (22). The natural frequencies are simplified as

$$\left.\begin{array}{l}_f\omega_n={}_s\omega_n+n\Omega\\ _r\omega_n=|{}_s\omega_n-n\Omega|\end{array}\right\}\quad n=0,\ 1,\ \cdots,\ N \quad (49)$$

Similarly, the critical speed is also simplified as

$$_c\Omega_n=\frac{{}_s\omega_n}{n},\ n=1,\ 2,\ \cdots,\ N \quad (50)$$

Figure 2 shows schematically the natural frequencies with the spinning speed when the strains remain nonlinear and the internal forces are linearized. The difference between the frequencies for the forward and reversed traveling waves is equal to when while it is equal to $2n\Omega$ when $0\leq\Omega\leq{}_c\Omega_n$ while it is equal to $2\sqrt{{}_s\omega_n^2+\Omega^2(\alpha_n+n^2\beta_n)}$ when $\Omega\geq{}_c\Omega_n$. On the other hand, the natural frequencies are shown in Fig. 3 as functions of when both the strains and internal forces linearized: in this case, the curves become straight lines on the diagram of the natural frequencies versus the spinning speed.

To verify the proposed approach, consider an example of a spinning disk whose material properties and physical dimensions are given in Table 1 except the inner radius which is given by 0. 0325 m. The natural frequencies of the stationary disk calculated by using the proposed approach are compared with the exact solutions (Mote, 1970). The results are summarized and compared in Table 2, where the differences between these two calculations are less than 0.3% so the results from the presented approach are acceptable.

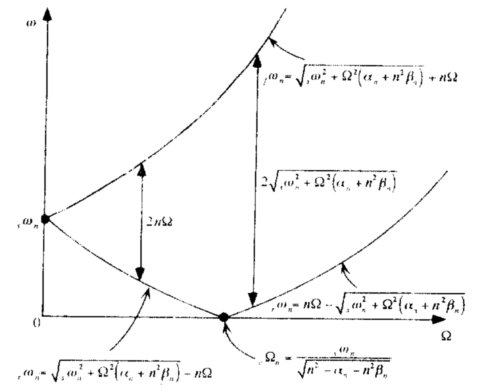

Fig. 2 Schematic diagram of the natural frequencies versus the spinning speed when the strains remain nonlinear while the internal forces are linearized ($n^2 \cdot \alpha_n \quad n^2\beta_n > 0$).

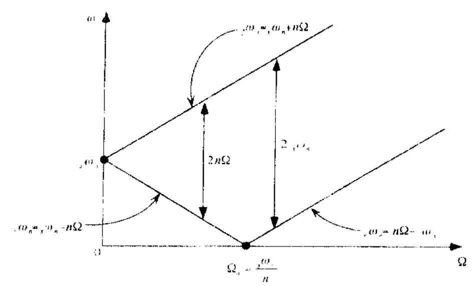

Fig. 3 Schematic diagram of the natural frequencies versus the spinning speed when both the strains and internal forces are linearized ($n \neq 0$).

Another verification is given by comparing the

Table 1 Material properties and dimensions of the spinning disk.

Material property/Dimension	Value
Young's modulus, E	65.5 MPa
Poisson's ratio, ν	0.3
Mass density, ρ	1200 kg/m^3
Thickness, h	0.0012 m
Inner radius, a	0.01742 m
Outer radius, b	0.065 m

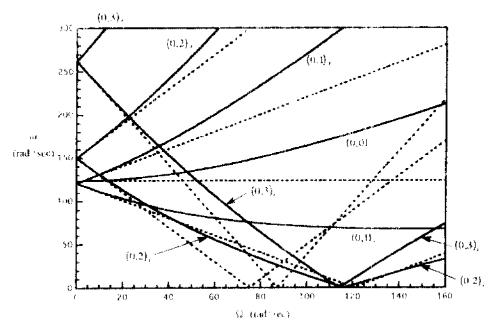

Fig. 4 Diagram of the natural frequencies versus the spinning speed.

Table 2 Comparison of the natural frequencies calculated by using the proposed method and the exact solutions when $\Omega = 0$ (rad/sec).

Mode (0, n)	(0, 0)	(0, 1)	(0, 2)	(0, 3)
Proposed method	261.61	267.05	295.83	373.59
Exact solutions	261.53	266.86	295.26	372.73
Error(%)	0.03	0.07	0.19	0.23

Table 3 Comparison of the critical speeds calculated by using the proposed method and Hutton's method (rad/sec).

Mode(0, n)	(0, 2)	(0, 3)	(0, 4)
Proposed method	116.35	114.28	140.58
Hutton's method	114.46	114.46	136.55
Error (%)	1.65	0.15	2.96

Table 4 Natural frequencies of the stationary disk and the nondimensional parameters.

Mode(0, n)	(0, 0)	(0, 1)	(0, 2)	(0, 3)
${}_s\omega_n$ (rad/sec)	261.61	267.05	295.83	373.59
α_n	2.2343	2.2353	2.2373	2.2367
β_n	0.1508	0.1507	0.1504	0.1501
$n^2-\alpha_n-n^2\beta_n$	−2.2343	−1.3859	1.1611	5.4124

critical speeds which are calculated with the proposed method and Hutton's method (Hutton, 1987). The material properties and dimensions are given by Table 1. Comparison of the critical speeds, shown in Table 3, leads to acceptance of the proposed method even though only the zero-nodal circle modes are chosen and they are assumed as simple comparison functions.

Figure 4 shows the well-known diagram of the natural frequencies versus the spinning speed of the disk whose mechanical properties and dimensions are given in Table 1. As discussed before, the dotted straight lines indicate the natural frequencies when both the strains and internal forces are linearized. In contrast, the solid curved lines indicate the natural frequencies when only the internal forces are linearized. The differences between them are so large that the natural frequencies expressed by the dotted straight lines are not acceptable.

It is interesting to examine the nature of natural frequency of the stationary disk and the nondimensional parameters. Table 4 shows numerical values for ${}_s\omega_n$, α_n, and β_n when the data of Table 1 are used. It can be seen that the values of α_n and β_n have very small variations for different numbers of the nodal diameters compared to ${}_s\omega_n$. It is also noted that there exists no critical speed, if the values of $n^2-\alpha_n-n^2\beta_n$ are less than or equal to zero: see Fig. 4 where the natural frequencies corresponding to (0, 0) and (0, 1) modes do not have a critical speed.

4. Conclusions

The governing equation for a spinning disk without a transverse load is analytically derived by using the variational formulation based upon the Kirchhoff plate theory and von Karman strain one. This approach is theoretically valid under the following two assumptions. The first assumption is that in-plane deflections are steady and axisymmetric with respect to the spinning disk center. The second one is that the strains are nonlinear functions of the displacements while the internal forces are linearized. In addition, the natural frequencies and the critical speeds of a freely spinning disk are examined with the natural frequency of the stationary disk, the number of nodal diameters, and the spinning speed.

In the future work, it is necessary to prove whether the steady and axisymmetric in-plane deflections are still valid or not even when transverse loads are applied to a spinning disk. In addition, it is interesting to investigate whether the totally coupled nonlinear governing equations can be obtained when either the strains or the internal forces remains nonlinear.

Acknowledgment

We would like to acknowledge support provided by Hanyang University for the first author.

References

Adams, G. G., 1987, "Critical Speed for a Flexible Spinning Disk," *International Journal of Mechanics,* Vol. 29, pp. 525∼531.

Benson, R. C., 1977, "Deflection of a Transversely loaded Spinning Disk," *Ph. D. Dissertation,* University of California, Berkeley.

Benson, R. C. and Bogy, D. B., 1978, "Deflection of a Very Flexible Spinning Disk due to a Stationary Transverse Load," *ASME Journal of Applied Mechanics,* Vol. 45, pp. 636∼641.

Chen, J. S. and Bogy, D. B., 1992, "Effects of Load Parameters on the Natural Frequencies and

Stability of a Flexible Spinning Disk with a Stationary Load System," *ASME Journal of Applied Mechanics,* Vol. 59, pp. 230～235.

Eversman, W., and Dodson, R. O., 1969, "Free Vibration of a Centrally Clamped Spinning Circular Disk," *AIAA Journal,* Vol. 7, No. 10, pp. 2010～2012.

Hutton, S. G., Chonan, S. and Lehmann, B. F., 1987, "Dynamic Response of a Guided Circular Saw," *Journal of Sound and Vibration,* Vol. 112 No. 3, pp. 527～539.

Iwan, W. D. and Moller, T. L., 1976, "The Stability of a Spinning Elastic Disk with a Transverse Load System," *ASME Journal of Applied Mechanics,* Vol. 43, pp. 485～490.

Lamb, H. and Southwell, R. V., 1921, "The Vibrations of a Spinning Disk," *Proceedings of the Royal Society,* Vol. 99, pp. 272～280.

Mote, Jr., C. D., 1965, "Free Vibration of Initially Stressed Circular Disks," *ASME Journal of Engineering for Industry,* Vol. 89, pp. 258～265.

Mote, Jr., C. D., 1970, "Stability of Circular Plates Subjected to Moving Loads," *Journal of the Franklin Institute,* Vol. 290, No. 4, pp. 329～344.

Ono, K., Chen, J. -S., Bogy, D. B., 1991, "Stability Analysis for the Head-Disk Interface in a Flexible Disk Drive," *ASME Journal of Applied Mechanics,* Vol. 58, pp. 1005～1014.

Shen, I. Y., 1993, "Response of a Stationary, Damped, Circular Plate under a Rotating Slider Bearing System," *ASME Journal of Vibration and Acoustics,* Vol. 115, pp. 65～69.